Gulati et al. Journal of Theoretical and Applied Physics 2012, 6:35
http://www.jtaphys.com/content/6/1/35

Journal of Theoretical and Applied Physics
a SpringerOpen Journal

RESEARCH **Open Access**

Diagnostic of plasma discharge parameters in helium filled dielectric barrier discharge

Pooja Gulati[1*], Udit Narayan Pal[1], Mahesh Kumar[1], Ram Prakash[1], Vishnu Srivastava[1] and Vimal Vyas[2]

Abstract

This paper reports the plasma discharge analysis of a dielectric barrier discharge (DBD) source. Helium is used as a working gas. The analysis is performed at fixed working pressure and operating frequency. The investigations are carried out using sinusoidal supply for the generation of discharges where two current pulses have been observed with different polarities in one period. A homogeneous type of discharge has been observed for different operating conditions in this DBD source. Since *in situ* diagnostics are not possible due to the small geometries in the used DBD source, the electrical measurements and spectroscopic analysis of the discharge have been performed to analyse the plasma discharge. The electrical analysis has been carried out using equivalent electrical circuit model. The plasma density and temperature within the discharge have been estimated using line ratio technique of the observed visible neutral helium lines. The estimated electron plasma density is found to be in close proximity with the plasma simulation code 'OOPIC Pro'.

Keywords: Dielectric barrier discharge, OOPIC pro, Line ratio, Particle in cell
PACS: 52.80.Hc, 52.65.Rr, 52.38.Hb, 52.70.Kz

Background

Dielectric barrier discharge (DBD) is an effective method for generating low temperature plasma at atmospheric pressure. Recently, much attention has been paid to the DBD technology due to its numerous industrial applications [1]. These types of plasma discharges are characterized by the presence of at least one insulating layer in contact with the discharge between two planar or cylindrical electrodes connected to an AC or pulse power supply [2]. The main advantage of such discharges is that non-equilibrium and non-thermal plasma conditions in atmospheric-pressure gases can be established in an economic and reliable way.

DBDs are mainly classified in three basic configurations. The first is the 'volume discharge' (VD) arrangement consisting of two parallel plates and any numbers of dielectric barriers in between the electrodes. The second configuration is the 'surface discharge' (SD) arrangement in which a plane dielectric with a number of surface electrodes on the dielectric layer and a counter electrode on its reverse side is used. In this configuration there is no clearly defined discharge gap. The third configuration is 'coplanar discharge' arrangement which is the combination of aforesaid two basic configurations [3,4]. In the present investigations, the volume discharge configuration has been used. The helium is used as the working gas because it has spectroscopic spectral analysis advantages [5].

The plasma discharges in most DBDs show filamentary and homogeneous (diffused type) discharges, which depend upon the experimental conditions such as gas type, pressure, electrodes gap, dielectric properties and applied voltage waveforms [6-12]. In fact the applied voltage waveform plays a key role in the discharge efficiency [13]. Nevertheless, the DBDs are driven traditionally by sine wave voltages with magnitudes in the kilovolt range and frequencies in the kilohertz range [14].

In the present work a barrier discharge using sinusoidal waveform at a working pressure 100 mbar in glow mode has been studied to understand the uniform mode operation of the discharge and also to identify corresponding discharge parameters. In the DBD discharges, the *in situ* diagnostics are not possible due to the small geometries, and passive diagnostics of DBDs became

* Correspondence: pgulati1512@gmail.com
[1]Microwave Tubes Division, Council of Scientific and Industrial Research-Central Electronics Engineering Research Institute (CSIR-CEERI), Pilani 333031, India
Full list of author information is available at the end of the article

important. For this the electrical model analysis and the spectroscopic diagnostic are the key possibilities that have been explored in this paper. The electrical analysis of the discharge has been performed using an equivalent electrical circuit model [14] and the dielectric voltage, gap voltage, memory voltage, discharge current, etc. are the parameters which have been obtained. The electron plasma density and temperature are measured using optical emission spectrometry (OES) diagnostic technique [15]. One of the OES methods is the line ratio technique, in which the intensity ratio of emission lines is related to electron plasma density and electron plasma temperature [16]. Spectroscopically, the DBD-based discharges are neither in local thermodynamical equilibrium nor in Coronal equilibrium regions and require the collisional-radiative (CR) model analysis for interpretation of the spectra [17]. In this work we report the plasma parameters of DBDs such as electron plasma temperature and electron plasma density by using the observed visible spectra of the helium neutral lines and CR model-based analysis. The electron density has been found almost identical with the obtained value from plasma simulation code OOPIC Pro [18].

Experimental details

Discharge geometry

The DBD geometry of the discharge consists of two parallel plate electrodes which are covered by the dielectric barriers made of quartz discs. Both the electrodes are made of copper of 3 mm thickness and 18 mm radius, while the quartz discs are 1 mm thick and 20 mm in radius. The space between the electrodes has been varied from 1.2 to 3.6 mm. The upper and lower electrode subassemblies are covered by Teflon to avoid long path arcing in the vacuum chamber. A sinusoidal signal is applied to the upper electrode and the lower electrode is kept grounded. Figure 1 shows a schematic view of the parallel plate geometry of the used DBD.

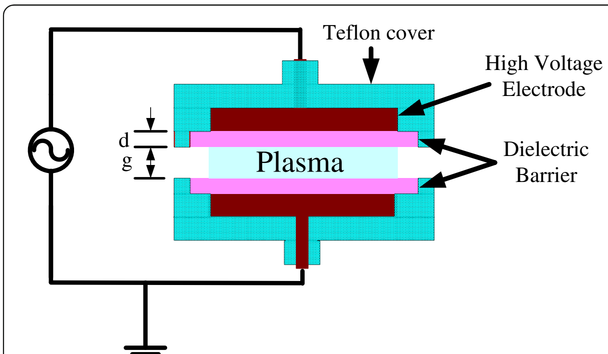

Figure 1 Schematic diagram of parallel plate DBD cell.

Experimental set-up

Figure 2 shows the schematic view of the experimental setup. A sinusoidal voltage is applied to the discharge electrodes for the generation of plasma discharge, and the source frequency is kept at 34.5 kHz. The DBD cell has been mounted inside the ultra high vacuum chamber. An Ocean Optics spectrometer (HR4000, Ocean Optics Inc., Dunedin, FL, USA) has been mounted with the vacuum chamber for the spectroscopic observations of the discharge. The vacuum chamber has been mounted on an ultra-high vacuum pump system using rotary and turbo molecular pumps. The base pressure is kept approximately 1×10^{-6} mbar. At room temperature, the helium gas of 99.9% purity (BOC Gases, BOC India Ltd. India) has been filled in the DBD cell. The pressure of the gas has been measured by pressure gauges (Pfeiffer APR262, Pfeiffer PKR251, Berliner Strasse, Asslar, Germany), and the pressure has been maintained by the vacuum valves (Matheson 316L, Matheson Trigas, Albuquerque, NM, USA; Varian 9515091, Varian Inc. Vacuum Technologies, CA, USA).

The upper copper electrode acts as anode which is connected to the high-voltage power supply (Huettinger HF Generator TIG 10/100 PSC, Huttinger Electronics Inc., Freiburg, Germany) comprising a frequency between 20 and 100 kHz, while the lower electrode is connected to the ground. A 1:1,000 high-voltage probe (Tektronix P6015A, Tektronix Inc., Beaverton, OR, USA) measures the voltage across the DBD, and the Rogowski-type Pearson current monitor, model 110 (Pearson Electronics, Inc., Palo Alto, CA, USA) (0.1VA-1, 1 Hz-20 MHz, 20 ns usable rise time), measures the total current flowing through the DBD. The total current and applied voltage waveforms are visualized by means of a four-channel Tektronix 4045 digital oscilloscope.

Results and discussion

Discharge mode and electrical analysis

The electrical behaviour of the discharge has been characterized by measuring the applied voltage and the discharge current. In the experiment the voltage applied to the upper electrode has been increased manually. When the applied voltage rose to a certain value V_{bd} (breakdown voltage), the discharge began with some filaments distributed on the dielectric wall, but the intensity of the visible light emitted from the discharge gap was very low. When the applied voltage is increased further, the number of filaments increased and finally gets diffused. Figure 3a shows the average image of the discharges, taken with a digital camera (SONY DSC-P100, exposure time 25 ms, SONY Electronics Inc., New York, NY, USA). Figure 3a shows the diffused structures of the filaments with the increasing voltage. The image illustrates that the diffuse discharge covers the entire surface

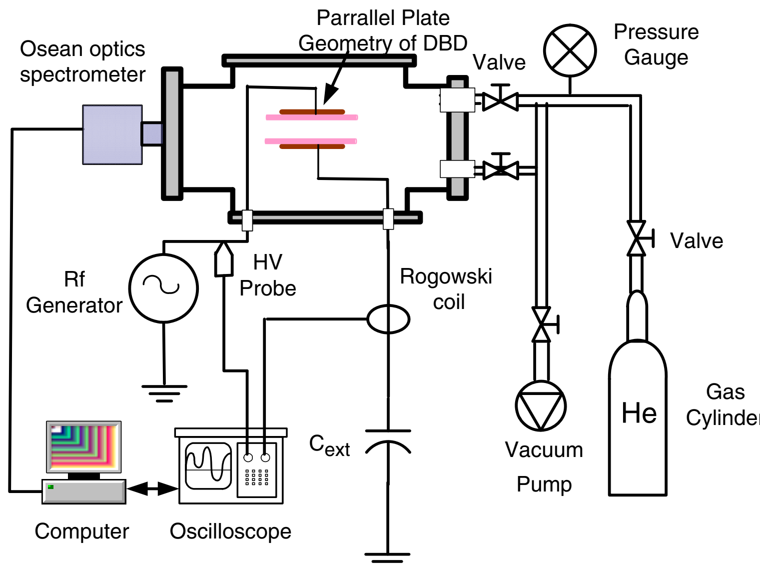

Figure 2 Schematic view of experimental arrangement.

of the electrodes. Figure 3b shows the total current trace together with the applied voltage. The visual inspection of the plasma and current waveform in Figure 3a,b reveals a uniform mode operation with homogeneous glow (under all operating conditions) which has filled essentially the entire gap between the dielectric-covered electrodes.

From the observed current-voltage waveforms and its equivalent circuit model [14] analysis, certain useful discharge parameters in the VD configuration in the DBD

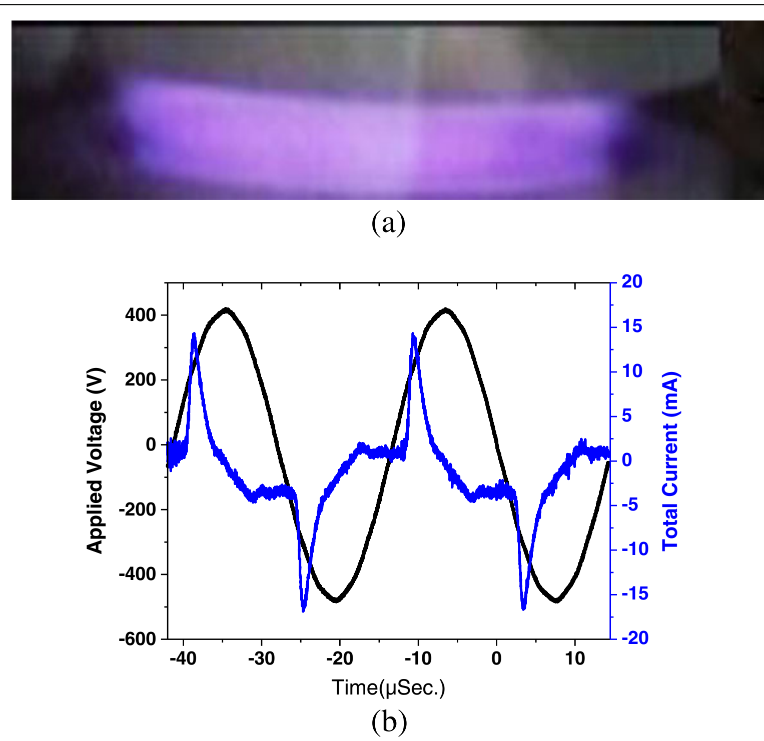

Figure 3 Helium gas discharge for 100 mbar at 34.5 kHz. (**a**) Camera view of diffuse discharge at 415V peak voltage and (**b**) applied voltage and total current waveform at 415V peak voltage.

discharge are obtained. The obtained internal temporal dynamic parameters are shown in Figure 4, which show the waveforms indicating the temporal behaviour of total applied voltage $V_a(t)$, total external current $I_{tc}(t)$ and estimated parameters specially memory voltage $V_m(t)$ (voltage due to the charge accumulated on the dielectric due to previous discharge), gas gap voltage $V_g(t)$, dielectric barrier voltage $V_d(t)$, the DBDs current $I_{dbd}(t)$ and conduction current $I_{dis}(t)$ at operating pressure of 100 mbar. To estimate these parameters in the equivalent electrical circuit model, the gap capacitance C_g and dielectric barrier capacitance C_d are used as input parameters and are obtained from the geometry of the configuration. The obtained values of C_g and C_d are 11.30 and 20.48 pF respectively.

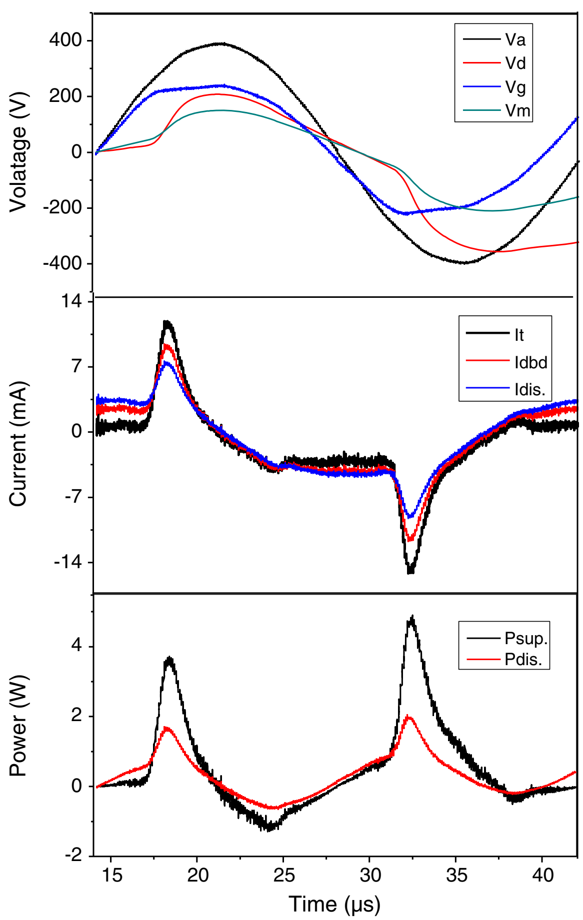

Figure 4 Experimental waveforms of dynamic processes occurring in gap. Experimental waveforms of dynamic processes occurring in gap (gas helium, frequency 34.5 kHz) for the parallel plate DBD geometry and at pressure 100 mbar. (**a**) Dynamic process in gap showing different voltage in gap, applied voltage V_a, dielectric voltage V_d, ,gap voltage V_g and memory voltage. (**b**) Total current I_t, DBD current I_{dbd}, current during discharge I_{dis}. (**c**) Applied power P_{sup} and power during discharge P_{dis}.

This figure indicates that the discharge occurs when the applied voltage reaches to the breakdown voltage (depending on the gap between the electrodes) which results in the significant electron production. The internal voltage or gap voltage, $V_g(t)$, rises with the external voltage until the primary discharge occurs. A small hump in the gap voltage marks the ignition condition. The discharge hump is corresponding to the weakening of the internal electric field in the gas gap due to the momentary flow of charges during the discharge. In the first half of the applied wave form, the discharge occurs due to the applied voltage which reaches the breakdown voltage. After that the produced electrons move towards the anode driven by gap voltage and reverse the polarity of the initial memory voltage. It is clearly evident from the figure that the gap voltage $V_g(t)$ attains a positive value prior to the applied voltage, which confirms the effect of the memory voltage.

The instantaneous power input $P_{sup}(t)$ has been estimated using

$$P_{\sup}(t) = V_a(t) \times I_{tc}(t). \tag{1}$$

The instantaneous power consumed or the discharge power by the plasma discharge in the gap has been obtained using

$$P_{dis}(t) = V_g(t) \times I_{dis}(t). \tag{2}$$

The obtained values of supplied power $P_{sup}(t)$ and consumed power $P_{dis}(t)$ corresponding to the applied waveforms are also shown in Figure 4. The positive half cycle of the applied voltage P_{sup} includes both the power dissipated in the gap during discharge and the reactive power stored in the various capacitors (cable, dielectric and gas). The real power input occurs during the discharge phase which shows that the external circuit provides the same power during both discharges. However, the consumed power in the second discharge is higher because the memory charges from the previous discharge that are deposited on the dielectric surface contribute to the energy consumed [10].

Spectroscopic analysis

The light emitted from the DBD source is fed to the compact ocean optics visible spectrometer (HR4000) using optical fibre for spectroscopic analysis. The time average spectra are recorded and are taken to the computer for further analysis and storage. This spectrometer uses grating 300 lines per millimetres and has spectrum bandwidth 2000-11000 Å along with the spectral resolution of approximately 0.75 nm. The typical spectrum of the used DBD is shown in Figure 5. A large number

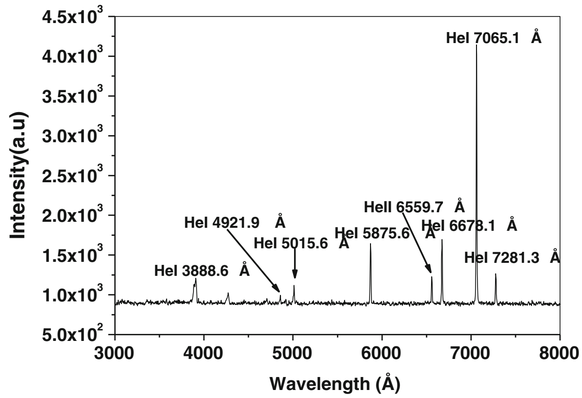

Figure 5 Observed helium neutral line spectra at working pressure. Observed helium neutral line spectra at working pressure 100 mbar, applied voltage 1,000 V and at frequency 34.5 kHz.

of neutral helium line emissions, like He I 3888.6 Å (2^3S-3^3P^0), He I 4921.9 Å (2^1P^0-4^1D), He I 5015.6 Å (2^1S-3^1P^0), He I 5875.6 Å (2^3P^0-3^3D), He I 6678.1 Å (2^1P-3^1D), He I 7065.1 Å (2^3P^0-3^3S) and He I 7281.3 Å (2^1P^0-3^1S) are observed from the plasma discharge. To estimate the electron plasma temperature and electron plasma density, a well-known line ratio technique is used [16] which do not require absolute intensity calibration of the spectrometer. For accurate estimations of plasma parameters, the CR model-based spectral analysis is essentially needed in the DBD sources [17]. So, we have derived relevant spectral line intensity ratios using CR model from the ADAS code [19].

In the CR model, the populations of various energy levels of atoms (or ions) in a plasma are calculated by assuming a quasi-steady-state exists among the excited levels, which depends on the plasma parameters N_e and T_e [19]. Accordingly, the intensities of the He I lines are calculated using CR model-based data from the ADAS database. With an assumption that the average electron density and temperature in an emission length x, the photon intensity $I(\lambda_{ul})$ of a spectral line can be written from the quasi-steady-state approximation of the CR model as [20]

$$\begin{aligned}\tilde{I}(\lambda_{ul}) &= PE\,\overline{C}_{recombining}\tilde{N}_e\left(\tilde{N}_i x\right)\\ &\quad + PE\overline{C}_{excitation}\tilde{N}_e\left(\tilde{N}_g x\right),\end{aligned} \tag{3}$$

where $PE—C_{recombining}$ and $PE—C_{excitation}$ represents the effective photon emission coefficients (photons per cubic centimetre per second) for recombination and excitation processes, respectively, in an average measurement. Here $\tilde{N}_g x$ and $\tilde{N}_i x$ are the average column densities of the ground state atoms (here referring to He I) and ions (here referring to He II). The ADAS code derives PEC values for a particular spectral line λ_{ul} after calculating the population distribution of levels. This is done by solving a set of coupled rate equations for the number of levels of the ionization stage i. In each equation, one includes all the processes of populating and depopulating the level by excitation, deexcitation, spontaneous emission, ionization and recombination from adjacent ionization stages, etc. [19]. The proportionality factors the effective photon emission coefficients (PECs) in Equation 3 are the functions of electron densities and temperatures only [20].

Under an ionizing plasma assumption [16,21], the first term in Equation 3 can be taken to be negligibly small and the line intensity $I(\lambda_{ul})$ for a transition from level u to level l is expressed as

$$\tilde{I}(\lambda_{ul}) = PE\,\overline{C}_{excitation}\tilde{N}_e\left(\tilde{N}_g x\right), \tag{4}$$

and the ratio of intensities of two lines becomes

$$\frac{I_{ul_1}}{I_{ul_2}} = \frac{PE\overline{C}_{excitation1}}{PE\overline{C}_{excitation2}}, \tag{5}$$

where I_{ul1} and I_{ul2} are the intensities of two spectral lines of a specific species of interest. The terms $PE—C_{excitation1}$ and $PE—C_{excitation2}$ are the corresponding PECs which are functions of N_e and T_e only. The other terms will be cancelled in the ratio output. Thus, it becomes easy to calculate the expected ratio of two lines under different plasma conditions of N_e and T_e. The line ratios that are sensitive to one of the quantities (either temperature or density) and insensitive to other quantity are useful to determine the required basic plasma parameters N_e and T_e. By using the density-sensitive singlet-singlet line pair 6678.1 Å (2^1P-3^1D)/ 7281.3 Å(2^1P-3^1S), we estimated $N_e = (3.5 \pm 1.5) \times 10^{11}$ cm^{-3} and by temperature sensitive singlet-triplet line pair of intensity ratio 7281.3 Å (2^1P-3^1S)/7065.1 Å (2^3P-3^3S) at 100 mbar working pressure, we obtained $T_e = 6.5 \pm 0.5$ eV. The existence of plasma density of approximately 10^{11} cm^{-3} is an indication for larger existence of metastable states [22] in the present DBD source which could be used as excimer light source [7].

Kinetic simulation

The 2D object-oriented particle in cell code OOPIC Pro (Tech-X Corp., Boulder, CO, USA) has been used to study the electrical as well as the kinetic behaviour of the DBDs [18]. The OOPIC Pro solves for the fields on the grid and calculates particle trajectories including self-consistently, the effects of charged particles on the fields with respect to the space and time variations. This also treats collision and ionization processes of a background neutral gas with Monte Carlo collisions method. Symmetrical 2D geometry of parallel plate DBD has been made as shown in Figure 6a, which also include the after effects of the discharge. In this model dark colour strips show the dielectric barriers and in between the gap, there is electron concentration after 125 ns time step where the simulation time step has been set at approximately 10^{-13} s by considering the relaxation time of DBD. All the operating conditions are kept similar to the experiment. An electrostatic field solver with time-dependent voltage has been applied to simulate the model. The electrostatic field solver neglects the magnetic field and electrodynamics effects so that we could isolate the effects of the electric field alone. Any sample of gas under normal conditions contains an average of 10^9 m^{-3} electrons and ions due to ultraviolet and cosmic radiations and radioactivity. So an electron density of approximately 10^9 m^{-3} is loaded uniformly in the gas gap along with the helium gas (100 mbar) to initiate the discharge at room temperature. A sinusoidal voltage is applied across the boundary to initiate the discharge.

The large number of filamentary discharge mixing after 125 ns time step is clearly visible in Figure 6a from the simulation, which can provide better understanding of the electron density of the diffused discharge if we observe the fluctuating density from its distribution. In fact the statistical mechanics have shown that the many small perturbation (errors) that affect a physical system almost always force the measurement to follow the Gaussian distribution as shown in Figure 6b. It is usually

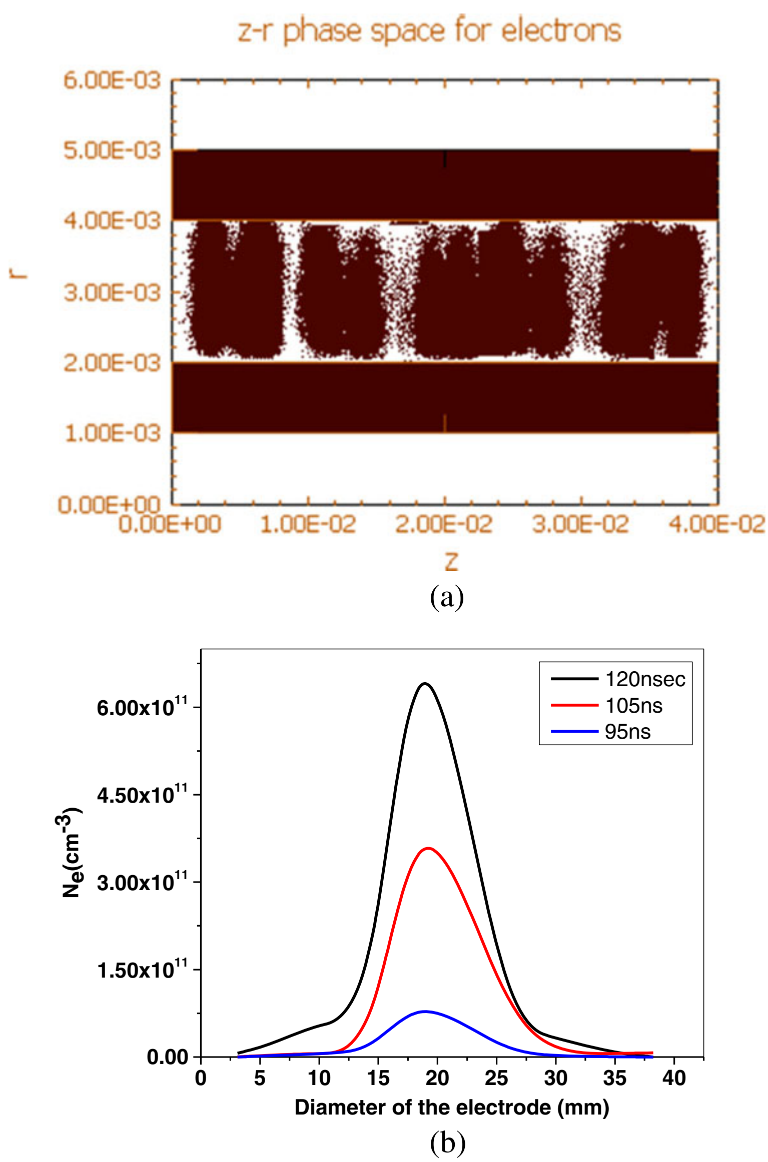

Figure 6 Parallel plate DBD simulations. (**a**) After discharge effects in the similar geometry of the experimental set-up. (**b**) Gaussian electron plasma density profile after discharge at different time steps.

referred to as simply the 'normal distribution'. Based on this, the average distribution of electron plasma density is derived for the entire system geometry using OOPIC Pro simulation code and when we take the average of the distributed density after 125 ns time step, it gives approximately $3.25 \times 10^{11}\ m^{-3}$. It has quite similar results to the spectroscopic diagnostic measurements which are in agreement with each other. It has been further observed that after 125 ns time step, the electron plasma density saturates and there is no further enhancement in the density.

Conclusions

The homogeneous type of discharge has been observed at working gas pressure 100 mbar and at a fixed frequency of 34.5 kHz in a parallel plate DBD geometry filled with helium gas. Two discharges are generated per single voltage cycle. The dynamic evolution of the process in the gap provides the useful information about the electrical characterization of the DBD source. The electron plasma temperatures and electron plasma density obtained for present VD configuration at 100 mbar gas pressure are typically 6.5 ± 0.5 eV and $3.5 \pm 1.5 \times 10^{11} cm^{-3}$ respectively, which is in close agreement with the simulated results.

Methods

In this paper, we have studied a dielectric barrier discharge plasma source, which has been designed and fabricated in parallel plate geometry of DBD. We performed the experiments for a fixed operating pressure at 100 mbar and took voltage and current waveform of the discharge. By using equivalent electrical model, we observed the dynamic processes of the discharge. Also, by using observed spectra and CR model-based analysis, we have estimated the basic plasma parameters such as electron plasma density and temperature in very thin geometry of the plasma. In such plasmas *in situ* diagnostics are not possible, and metallic probe diagnostics can lead erroneous results due to sheath-sheath interaction process. The obtained plasma parameters have been validated with the kinetic simulation results using PIC code.

Competing interests

The authors declare that they have no competing interests.

Authors' contributions

PG participated in carrying out the experiments, simulation and drafted the manuscript. UNP actively participated in the experiments. RP conceived the study and participate in CR model analysis. MK gave technical support in the experiments. VS and VV participated in sequence alignment. All authors read and approved the final manuscript.

Acknowledgements

The work has been carried out under CSIR Network Programme. The authors are grateful to Dr. Chandra Shekhar, Director of CEERI Pilani and also Dr. S. N. Joshi, Emeritus Scientist, in CEERI, Pilani for the useful scientific discussions and support.

Author details

[1]Microwave Tubes Division, Council of Scientific and Industrial Research-Central Electronics Engineering Research Institute (CSIR-CEERI), Pilani 333031, India. [2]Department of Physics, Banasthali University, Banasthali, Jaipur, Rajasthan 304022, India.

Received: 30 October 2012 Accepted: 30 October 2012
Published: 22 November 2012

References

1. Boricia, G, Dumitrascu, N, Popa, G: Influence of helium-dielectric barrier discharge treatments on the adhesion properties of polyamide-6 surfaces. Surf. Coat. Tech. **197**, 316–321 (2005)
2. Liu, S, Neiger, M: Electrical modeling of homogeneous dielectric barrier discharge under an arbitrary excitation voltage. J. Phys. D: Appl. Phys. **36**, 3144–3150 (2003)
3. Gibalov, IV, Pietsch, GJ: The development of dielectric barrier discharges in gas gaps and on surfaces. J. Phys. D: Appl. Phys. **33**, 2618 (2000)
4. Beleznai, S, Mihajlik, G, Maros, I, Balázs, L, Richter, P: High frequency excitation waveform for efficient operation of a xenon excimer dielectric barrier discharge lamp. J. Phys. D: Appl. Phys. **43**, 015203 (2010)
5. Prakash, R, Jain, J, Kumar, V, Manchanda, R, Agarwal, B, Chowdhuri, MB, Banerjee, S, Vasu, P: Calibration of a VUV spectrograph by collisional-radiative modelling of a discharge plasma. J. Phys. B-At. Mol. Opt. **43**, 144012 (2010)
6. Radu, I, Bartnikas, R, Czeremuszkin, G, Wertheimer, M: Diagnostics of dielectric barrier discharges in noble gases: atmospheric pressure glow and pseudoglow discharges and spatio-temporal patterns. IEEE Trans. Plasma Sci. **31**, 411–421 (2003)
7. Roth, JR, Rahel, J, Dai, X, Sherman, DM: The physics and phenomenology of one atmospheric uniform glow discharge plasma (OAUGDP™) reactors for surface treatment applications. J. Phys. D: Appl. Phys. **38**, 555–567 (2005)
8. Rahel, J, Sherman, DM: The transition from a filamentary dielectric barrier discharge to a diffuse barrier discharge in air at atmospheric pressure. J. Phys. D: Appl. Phys. **38**, 547–554 (2005)
9. Gherardi, N, Massines, F: Mechanisms controlling the transition from glow silent discharge to streamer discharge in nitrogen. IEEE Trans. Plasma Sci. **29**, 536–544 (2001)
10. Massines, F, Rabehi, A, Decomps, P, Gadri, RB, Ségur, P, Mayoux, C: Experimental and theoretical study of a glow discharge at atmospheric pressure controlled by dielectric barrier. J. Appl. Phys. **83**, 2950–2957 (1998)
11. Massines, F, Ségur, P, Gherardi, N, Khamphan, C, Ricard, A: Physics and chemistry in a glow dielectric barrier discharge at atmospheric pressure: diagnostic and modeling. Surf. Coat. Technol. **174–175**, 8–14 (2003)
12. Okazaki, S, Kogoma, M, Uehara, M, Kimura, Y: Appearance of stable glow discharge in air, argon, oxygen and nitrogen at atmospheric pressure using a 50 Hz source. J. Phys. D: Appl. Phys. **26**, 889–992 (1993)
13. Pal, UN, Gulati, P, Kumar, N, Kumar, M, Tyagi, MS, Meena, BL, Sharma, AK, Prakash, R: Analysis of discharge parameters in xenon-filled coaxial DBD tube. IEEE Trans. Plasma Sci. **39**, 1475–1481 (2011)
14. Pal, UN, Sharma, AK, Soni, JS, Kumar, S, Khatun, H, Kumar, M, Meena, BL, Tyagi, MS, Lee, BJ, Iberler, M, Jacoby, J, Frank, K: Electrical modelling approach for discharge analysis of a coaxial DBD tube filled with argon. J. Phys. D: Appl. Phys. **42**, 045213 (2009)
15. Hutchinson, IH: Principles of Plasma Diagnostics. Cambridge University Press, Cambridge (2002)
16. Prakash, R, Vasu, P, Kumar, V, Manchanda, R, Chowdhuri, MB, Goto, M: Characterization of helium discharge cleaning plasmas in ADITYA tokamak using collisional-radiative model code. J. Appl. Phys. **97**, 043301–043307 (2005)
17. Srivastava, AK, Garg, MK, Prasad, KSG, Kumar, V, Chowdhuri, MB, Prakash, R: Characterization of atmospheric pressure glow discharge in helium using Langmuir probe, emission spectroscopy, and discharge resistivity. IEEE Trans. Plasma Sci. **35**, 1135–1142 (2007)
18. OOPIC Pro, Tech X Corporation: OOPIC-Pro User guide. http://www.techxcorp.com
19. Summers, HP: ADAS Users Manual JET-IR 06. JET Joint Undertaking, Abingdon (1994)
20. Agarwal, B, Prakash, R, Jain, J, Kumar, V, Vasu, P: Boron spectral line ratios helpful to characterize wall conditioned tokamak plasmas. Phys. Scr. **80**(055505), 1–5 (2009)

21. Goto, M: Determination of the hydrogen and helium ion densities in the initial and final stages of a plasma in the large helical device by optical spectroscopy. J. Quant. Phys. Plasmas **10**, 1402–1410 (2003)
22. Nersisyan, G, Morrow, T, Graham, WG: Measurements of helium metastable density in an atmospheric pressure glow discharge. Appl. Phys. Lett. **85**, 1487–1489 (2004)

doi:10.1186/2251-7235-6-35
Cite this article as: Gulati *et al.*: **Diagnostic of plasma discharge parameters in helium filled dielectric barrier discharge.** *Journal of Theoretical and Applied Physics* 2012 **6**:35.